THERMODYNAMIC ANALYSIS OF A NOVEL SOLAR CENTRAL RECIEVER MULTIGENERATION SYSTEM WITH HYDROGEN PRODUCTION

Muhammad Abid[1*], Victor Adebayo[1] Ugur Atikol[2]
[1] Cyprus International University, Faculty of Engineering, Department of Energy Systems Engineering, Nicosia, North Cyprus Via Mersin 10, Turkey
[2] Eastern Mediterranean University, Faculty of Engineering, Department of Mechanical Engineering, Famagusta, North Cyprus Via Mersin 10, Turkey
[*]Corresponding author e-mail: mabid@ciu.edu.tr

REFERENCE NO

MULT-04

Keywords:
Absorption chiller; Rankine; Brayton; Multigeneration; Exegetic

ABSTRACT

In this paper, a novel solar driven multigeneration system integrated with thermal storage is designed and analyzed for electricity, cooling, hot water and hydrogen production. The multigeneration system consists of a solar central receiver which utilizes molten salt (46.5%LiF11.5%NaF42%KF) as heat transfer fluid, a Brayton cycle, a Rankine cycle, an organic Rankine cycle (ORC), an absorption chiller (AC), domestic water heating system, an electrolyzer and thermal energy storage system. Thermodynamic analysis using the energy and exergy approach is performed to examine the multigeneration system, its subsystems and to observe its performance. The overall system energetic and exegetic efficiencies is found to be 49.74% and 27.12% respectively. The COP and exegetic efficiency of the AC is found to be 0.8427 and 0.3454 respectively. The effects of changing some system operating conditions on the efficiencies of the overall system and its subsystems are also studied.

1. INTRODUCTION

As the energy demand is increasing all over the world, many negative effects are caused on the environment due to specially fossil fuel-usage. Fossil fuels that contain carbon account for about 87% of the carbon emissions generated by humans [1]. Renewable energy sources, like solar energy and wind energy can provide solutions to the issues encountered with the use of fossil fuels. The only set back with the use of renewable energy sources is their low efficiencies. The periodical nature of solar energy (due to winter periods, cloudy days and night time) has made solar power systems have low performance and capacity factor. Incorporating the use of thermal storage; using molten salt for example will lead to great investment cost for setting up a particular solar power plant [2]. On the other hand multigeneration can provide solutions to improve the efficiencies of these renewable energy-based power generating systems.

Many studies have been conducted on multigeneration energy systems. Dincer et al. [3] performed an analysis using renewable energy for a system and found that its exergy efficiencies ranged from 55% to 65%, reliant on the extent of cogeneration involved. Khalid et al. [4] performed a thermodynamic analysis of a cogeneration system based on gas turbine and adsorption refrigeration chiller system, some parametric studies of the effects of exhaust gas admittance temperature for Brayton turbine, the composition of exhaust gas on the first and second law efficiencies, and exergy destruction for the cogeneration system and its components. Ozlu et al.[5] proposed a multigeneration energy system based on renewable energy resources for residential buildings and multi-building complex. The maximum energy efficiency was found to be 57% and the maximum exergy efficiency 36%. Maximum power and maximum cooling effect was found to be 92kW and 128kW. CO_2 reduction by this system was found to be 1398 tons per year. In Ref. [6] a multigeneration system was designed to integrate a gas turbine driven by solar with organic Rankine cycle. The energy

and exergy efficiencies of the multigeneration system was found to be 28.4% and 27% respectively. [7] proposed a novel system consisting of a heliostat field, gas cycle and a re-heat steam cycle, capable of producing power and hot water simultaneously. Thermodynamic analysis was performed on the system to access its performance energetically and exegetically. The literature above suggests that multigeneration systems may be a beneficial option to subdue the issue of global warming, which has been an issue of concern in the world today, and also raise the efficiency of any energy system. The present study is concerned with the energy and exergy analysis of six energy systems integrated in a multigeneration system. The objective is to use solar energy as the primary energy source with a central receiver using molten salt (46.5%LiF11.5%NaF42%KF) as HTF. It is rare to find six different energy systems integrated in one system in the literature. Therefore, this study is an interesting and novel addition to science.

2. SYSTEM DESCRIPTION

The proposed multigeneration system (fig 1) is driven by solar energy. It consists of a Bryton cycle, a Rankine cycle, an organic Rankine cycle, an absorption chiller, an electrolyser and a domestic hot water system. The basic outputs of this proposed system are electricity, cooling, heating and hydrogen production. The major part of the system is the solar central receiver system (heliostat field system)through which energy from the sun is trapped and converted into thermal energy. The heliostat tracks the sun to concentrate the sunlight rays on the solar receiver which contains molten salt (46.5%LiF11.5%NaF42%KF). At state a, part of the heated molten salt enters the hot storage tank and the other part is sent to the first heat exchanger during the day when there is sunlight to heat the compressed air in the Brayton Cycle. The cooled molten salt returns part receiver (state b), but at night it returns to the cold storage tank. The gas cycle is made up of three components; a compressor, a heat exchanger and a turbine. In this parametric study, air was chosen as the working fluid in the gas cycle. At state 1, fresh air enters the compressor and it is compressed. Its pressure and temperature increase at state 2 (exit of the compressor). Air is then heated by the heat coming from the solar central receiver. This is done in the heat exchanger I, this increases the pressure and temperature of air further to a very high value. This air then enters the gas turbine at state 3, thereby causing it to rotate and produce power. The exhaust gas from the Gas turbine is then used to drive the reheat-Rankine cycle using a heat exchanger and the remaining heat is used for to run an isobutane organic Rankine cycle. The reheat-Rankine cycle is composed of five parts; a pump, a heat exchanger, high-pressure turbine (HPT), a low-pressure turbine (LPT) and a condenser; the condenser acts as a heat exchanger. At state 9 water enters the pump and then moves to state 10 it goes through the heat exchanger II where it is being heated. At state 5 it turns to steam and enters the turbine; the fluid is then passed through the heat exchanger II at state 6 to be reheated again, and then passed to LPT at state 7 to produce work. The remaining heat is then passed through heat exchanger III at state 8 where it is used to drive the generator of the single effect absorption chiller. LiBr-water is the working fluid selected for the absorption chiller. Heat is transferred from heat exchanger III to the generator of the absorption chiller, before entering the pump of the steam cycle. After this heat is been received, a part of the water in the generator evaporates and enters the condenser at state 18. The water vapor is cooled down in the condenser at state 19, converting it back to water and throttled in the expansion valve. The temperature off the water drops as it enters the evaporator at state 20. When the cooling load is absorbed in the evaporator, the water is vaporized and enters the absorber where it mixes with the lean mixture of LiBr-water coming from the generator through heat exchanger IV and the expansion valve. It is then converted to a rich mixture of LiBr-water. At state 12 the mixture is pumped by the aid of the pump to the generator through the heat exchanger IV.

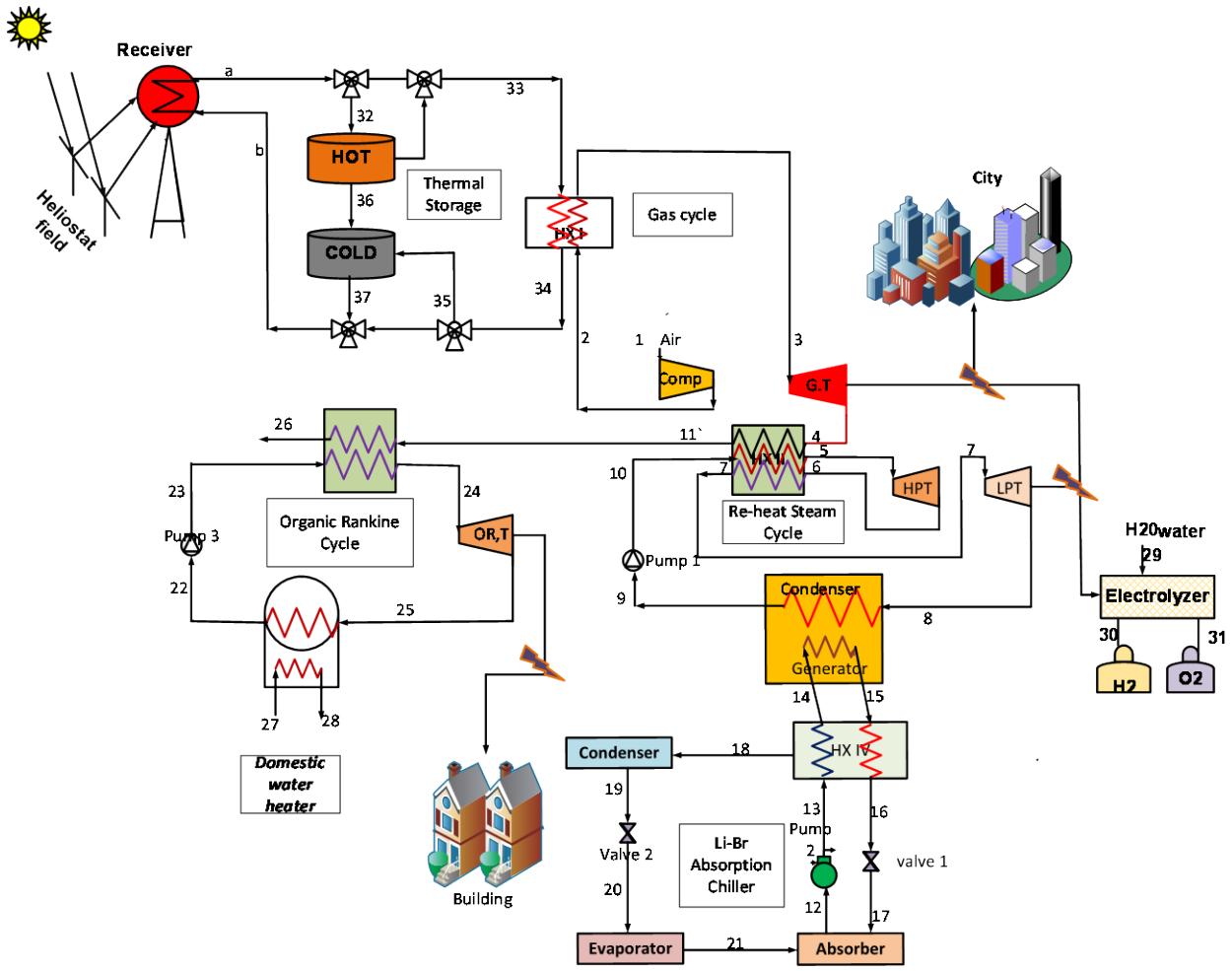

Figure 1: Schematic illustration of the solar multigeneration system

3. METHODOLOGY

In this research, thermodynamic analysis is performed and it is done by solving energy and exergy balance equations in Engineering Equation Solver (EES). In order to access the performance of the overall system and its subsystems, the energy and exergy efficiencies are determined also the energy and exergy inputs and outputs and the rate of irreversibility are determined.

3.1. Energy and Exergy Analysis

The energy and exergy balances for major components of the system are shown in this section. Some assumptions were made while the analysis was being carried out to simplify things and make it easier for steady state analysis to be performed. Some of the assumptions made are as follows:

- Air is treated as an ideal gas
- Reference state for the environment has a temperature of 298K and environmental pressure of 101.325 kPa
- The changes in kinetic and potential energy and exergy are negligible.
- Pressure loss in all the pipelines are negligible.
- The system is running at a steady state condition with constant solar insolation.

3.1.1 Solar block

The model used in the modelling of the solar power tower is that presented by [8].

The rate of heat received via solar irradiation is given as:

$$\dot{Q}_{sol} = I \times A_{field} \quad (1)$$

I, is the region's solar light intensity and A_{field} is the area of the heliostat field. The rate of heat received by the central receiver is gotten using:

$$\eta_H = \frac{\dot{Q}_{rec}}{\dot{Q}_{sol}} \quad (2)$$

Where η_H is the heliostat field efficiency, $\dot{Q}_{rec}$ is the rate of heat gained by the central receiver, and $\dot{Q}_{sol}$ is the rate of heat received by the solar irradiation. The emissivity of the central receiver is defined as:

$$\varepsilon_{avg} = \frac{\varepsilon_w}{\varepsilon_{w+(1-\varepsilon_w)F_r}} \quad (3)$$

ε_w stands for the emmisivity of the central receiver wall, and F_r is the view factor. The receiver's inner side temperature is given as:

$$T_{insi} = \frac{T_{rec,surf}+T_O}{2} \quad (4)$$

$T_{rec,surf}$ is the temperature of the receiver's surface and T_o represents the ambient temperature of the surrounding environment. Surface area and aperture area of the central receiver are both calculated as:

$$A_{rec,surf} = \frac{A_{field}}{C \times F_r} \quad (5)$$

Aperture area is given as:

$$A_{ap} = \frac{A_{field}}{C} \quad (6)$$

A_{field} is the area of the collector field, C stands for the concentration ratio, while F_r stands for the view factor. Heat loss rate in the central receiver because of emissivity is given by:

$$\dot{Q}_{rec,em} = \frac{\varepsilon_{avg}\sigma(T^4_{rec,surf}-T^4_O)A_{field}}{C} \quad (7)$$

σ represents Stefan-Boltzmann constant. The rate of heat loss in the central receiver due to reflection is given as:

$$\dot{Q}_{rec,ref} = \dot{Q}_{rec}\,\rho F_r \quad (8)$$

The rate of heat loss in the central receiver because of convection is calculated using:

$$\dot{Q}_{rec,em} = \frac{\varepsilon_{avg}\sigma(T^4_{rec,surf}-T^4_O)A_{field}}{C} \quad (9)$$

$h_{air,fc,insi}$ and $h_{air,nc,insi}$ are the forced and natural convective heat transfer coefficients of the inside of the receiver, respectively. The rate of heat loss in the central receiver due to conduction is given as:

$$\dot{Q}_{rec,cond} = \frac{(T_{rec,surf}-T_O)A_{field}}{\left(\frac{\delta_{insu}}{\lambda_{insu}}+\frac{1}{h_{air,o}}\right)(C \times F_r)} \quad (10)$$

δ_{insu} represents the insulation thickness, λ_{insu} is the thermal conductivity of insulation, $h_{air,o}$ is the convection heat transfer coefficient of the air outside. The convection heat transfer coefficient of air is composed of two parts, which is the natural and the forced coefficients:

$$h_{air,o} = h_{air,nc,,o} + h_{air,fc,o} \quad (11)$$

Heat rate absorbed by the molten salt HTF (heat transfer fluid) passing through the central receiver is given as:

$$\dot{Q}_{rec,abs} = \dot{m}_{ms}C_p(T_{ms,o} - T_{ms,in}) \quad (12)$$

$\dot{m}_{ms}$ is the mass flow rate of molten salt, c_p is the specific heat capacity of molten salt while $T_{ms,o}$ and $T_{ms,in}$ are the temperatures of molten salt leaving and entering the receiver respectively. So therefore, the total hat trapped by the receiver is determined by:

$$\dot{Q}_{rec}=\dot{Q}_{rec,em}+\dot{Q}_{rec,ref}+\dot{Q}_{rec,conv}+\dot{Q}_{rec,cond}+\dot{Q}_{rec,abs} \quad (13)$$

The temperature of the central receiver is determined by:

$$\frac{\dot{Q}_{rec}}{\frac{A_{field}}{FrXC}} = \frac{T_{insu,w}-T_{ms}}{\frac{d_o}{d_o \times h_{ms}} + d_o\left(\frac{In\left(\frac{d_o}{d_i}\right)}{2\lambda_{tube}}\right)} \quad (14)$$

d_o and d_o are the outer and inner diameters of the absorber tube, T_{ms} is the mean temperature of molten salt, λ_{tube} represents the conductivity of the absorber tube and h_{ms} is convection heat transfer coefficient. The energy efficiency of the heliostat field is given as :

$$\eta_H = \frac{\dot{Q}_{rec}}{\dot{Q}_{sol}} \quad (15)$$

The exergy associated with solar irradiation on the heliostat mirror surface ($\dot{E}x_s$) can be expressed as:

$$\dot{E}x_s = \left(1 - \frac{T_O}{T_{sun}}\right) \times \dot{Q}_{sol} \quad (16)$$

T_{sun} is the sun temperature. The exergy delivered to the receiver is given as:

$$\dot{E}x_{rec} = (1 - \frac{T_O}{T_{sun}}) \times \dot{Q}_{rec} \quad (17)$$

Exergy efficiency of heliostat field is given as:

$$\eta_{ex_H} = \frac{\dot{E}x_{rec}}{\dot{E}x_s} \quad (18)$$

The energy and exergy balance of the receiver is given as:

$$\dot{Q}_{rec} = \dot{Q}_{rec,abs} + \dot{Q}_{rec,totloss} \quad (19)$$

$$\dot{E}x_{rec} = \dot{E}x_{rec,abs} + \dot{E}x_{rec,totloss} \quad (20)$$

The thermal energy efficiency of the receiver is determined from:

$$\eta_{En_{rec}} = \frac{\dot{Q}_{rec,abs}}{\dot{Q}_{rec}} \quad (21)$$

Exergy efficiency of the receiver is:

$$\eta_{\dot{E}x_{rec}} = \frac{\dot{E}x_{rec,abs}}{\dot{E}x_{rec}} \quad (22)$$

3.1.2. Gas Cycle (Brayton Cycle)

Energy and exergy balances for the Gas cycle are given below:

Compressor:

Energy balance

$$\dot{W}_c + \dot{m}_1 h_1 = \dot{m}_1 h_2 \quad (23)$$

Exergy balance:

$$\dot{E}x_{destC} + \dot{E}x_1 = \dot{E}x_2 + \dot{W}_c \quad (24)$$

Table 1 Properties of the central receiver

Parameter	Symbol	Values
Total heliostat area	A_{field}	10,000m^2
Central receiver aperture area	$A_{rec,surf}$	12.5m^2
Heliostat efficiency	η_H	75%
Inlet temperature of molten salt	$T_{ms,i}$	750K
Outlet temperature of molten salt	$T_{ms,o}$	1350K
View factor	F_r	0.8
Tube diameter	d	0.019m
Tube thickness	t	0.00165m
Emissivity	ε_w	0.8
Wind velocity	V	5m/s
Insulation thickness	λ_{insu}	0.07m
Concentration ratio	C	1000

Heat Exchanger I (Molten salt to air heat exchanger):

Energy balance:

$$\dot{Q}_{rec,abs} = \dot{m}_3 h_3 - \dot{m}_2 h_2 \quad (25)$$

Exergy balance:

$$\dot{E}x_2 + \dot{E}x_{th}HXI = \dot{E}x_3 + \dot{E}x_{destHXI} \quad (26)$$

Gas Turbine:

Energy balance:

$$W_T + \dot{m}_4 h_4 = \dot{m}_3 h_3 \quad (27)$$

Exergy balance:

$$\dot{E}x_3 + \dot{W}_{GT} = \dot{E}x_4 + \dot{E}x_{destGT} \quad (28)$$

The thermal efficiency of the Gas cycle is given as:

$$\eta_{GC} = \frac{W\,net_G}{\dot{Q}_{rec,abs}} \quad (29)$$

3.1.3. Steam (Rankine Cycle)

Energy and exergy balances for the Steam Cycle are given below:

Pump I:

Energy balance:

$$\dot{m}_{10} h_{10} = \dot{m}_9 h_9 + \dot{W}_{P1} \quad (30)$$

Exergy balance:

$$\dot{E}x_9 + \dot{W}_{P1} = \dot{E}x_{10} + \dot{E}x_{destP1} \quad (31)$$

Heat Exchanger II:

Energy balance:

$$\dot{Q}_{HXII} = \dot{m}_5 h_5 - \dot{m}_{10} h_{10} + \dot{m}_7 h_7 - \dot{m}_6 h_6 \quad (32)$$

Exergy balance:

$$\dot{E}x_{10} + \dot{E}x_6 + \dot{E}x_{th}HXII = \dot{E}x_5 + \dot{E}x_7 + \dot{E}x_{destHXII} \quad (33)$$

Low pressure turbine (LPT):

Energy balance:

$$\dot{W}_{LPT} + \dot{m}_8 h_8 = \dot{m}_7 h_7 \quad (34)$$

Exergy balance:

$$\dot{E}x_7 + \dot{W}_{LPT} = \dot{E}x_8 + \dot{E}x_{destLPT} \quad (35)$$

High pressure turbine (HPT):

Energy balance:

$$\dot{W}_{HPT} + \dot{m}_6 h_6 = \dot{m}_5 h_5 \quad (36)$$

Exergy balance:

$$\dot{E}x_5 + \dot{W}_{HPT} = \dot{E}x_6 + \dot{E}x_{destHPT} \quad (37)$$

Condenser I:

Energy balance:

$$\dot{Q}_{Cond1} + \dot{m}_9 h_9 = \dot{m}_8 h_8 \quad (38)$$

Exergy balance:

$$\dot{E}x_8 = \dot{E}x_9 + \dot{E}x_{th}Cond_1 + \dot{E}x_{destcond1} \quad (39)$$

The thermal efficiency of the steam cycle is given as:

$$\eta_{ST} = \frac{W\,net_{ST}}{\dot{Q}_{HXII}} \quad (40)$$

The thermal efficiency of the Combined Cycle is given as:

$$\eta_{ST} = \frac{W\,net_{CS}}{\dot{Q}_{rec,abs}} \quad (41)$$

3.1.4. Single Effect Absorption Cycle

Energy and exergy balances for the Single Effect Absorption Refrigeration Cycle is

Pump II:

Energy balance:

$$\dot{W}_{P2} + \dot{m}_{12} h_{12} = \dot{m}_{13} h_{13} \quad (42)$$

Exergy balance:

$$\dot{E}x_{12} + \dot{W}_{P2} = \dot{E}x_{13} + \dot{E}x_{destPump2} \quad (43)$$

Generator:

Energy balance:

$$\dot{Q}_{GEN} + \dot{m}_{14} h_{14} = \dot{m}_{18} h_{18} + \dot{m}_{15} h_{15} \quad (44)$$

Exergy balance:

$$\dot{E}x_{12} + \dot{E}x_{th}GEN = \dot{E}x_{15} + \dot{E}x_{18} + \dot{E}x_{destGEN} \quad (45)$$

Condenser II:
Energy balance:
$\dot{Q}_{Cond2} + \dot{m}_{19}h_{19} = \dot{m}_{18}h_{18}$ (46)
Exergy balance:
$\dot{E}x_{18} = \dot{E}x_{19} + \dot{E}x_{th}Cond2 + \dot{E}x_{destcond2}$ (47)
Refrigerant Valve I:
Energy balance:
$\dot{m}_{19}h_{19} = \dot{m}_{20}h_{20}$ (48)
Exergy balance:
$\dot{E}x_{19} = \dot{E}x_{20} + \dot{E}x_{destrefv1}$ (49)
Evaporator:
Energy balance:
$\dot{Q}_E + \dot{m}_{20}h_{20} = \dot{m}_{21}h_{21}$ (50)
Exergy balance:
$\dot{E}x_{20} + \dot{E}x_{th}E = \dot{E}x_{21} + \dot{E}x_{destE}$ (51)
Absorber:
Energy balance:
$\dot{Q}_A + \dot{m}_{12}h_{12} = \dot{m}_{17}h_{17} + \dot{m}_{21}h_{21}$ (52)
Exergy balance:
$\dot{E}x_{21} + \dot{E}x_{17} = \dot{E}x_{destA} + \dot{E}x_{th}A + \dot{E}x_{12}$ (53)
Refrigerant Valve II:
Energy balance:
$\dot{m}_{16}h_{16} = \dot{m}_{17}h_{17}$ (54)
Exergy balance:
$\dot{E}x_{16} = \dot{E}x_{17} + \dot{E}x_{destrefv2}$ (55)
Heat Exchanger IV:
Energy balance:
$\dot{m}_{13}h_{13} + \dot{Q}_{HXIV} = \dot{m}_{14}h_{14}$ (56)
Exergy balance:
$\dot{E}x_{13} + \dot{E}x_{th}HXIV = \dot{E}x_{14} + \dot{E}x_{destHXIV}$ (57)

The energy Coefficient of performance for the single effect absorption refrigeration cycle is given as:
$Cop_{en} = \frac{\dot{Q}_E}{(\dot{Q}_{GEN} + \dot{Q}_{Pump})}$ (58)
For the exergy Coefficient of performance, is given as:
$Cop_{ex} = \frac{\dot{E}x_{th}E}{\dot{E}x_{th}GEN}$ (59)

3.1.5. Organic Rankine Cycle

Pump III:
Energy balance:
$\dot{W}_{P3} + \dot{m}_{22}h_{22} = \dot{m}_{23}h_{23}$ (60)
Exergy balance:
$\dot{E}x_{22} + \dot{W}_{P3} = \dot{E}x_{23} + \dot{E}x_{destPump3}$ (61)
ORC turbine:
Energy balance:
$\dot{W}_{ORC} + \dot{m}_{25}h_{25} = \dot{m}_{24}h_{24}$ (62)
Exergy balance:
$\dot{E}x_{24} + \dot{W}_{ORC} = \dot{E}x_{25} + \dot{E}x_{destORC,T}$ (63)
Heat exchanger IV:
Energy balance:
$\dot{Q}_{hx,orc} = \dot{m}_{11}(h_{11} - h_{26}) + \dot{m}_{24}(h_{24} - h_{23})$ (64)
The thermal efficiency of the organic Rankine cycle is given as:
$\eta_{ST} = \frac{\dot{W}_{ORC}}{\dot{Q}_{hx,orc}}$ (65)

3.1.6. Electrolyser

The chemical reaction for water electrolysis is:

$H_20 \xrightarrow{\text{Electricity}} H2 + \frac{1}{2}O_2$

It shows he number of moles of hydrogen that is produced for a given number of moles of water. The hydrogen production rate is determined using the commercial definition of electrolyser efficiency:

$\eta_{electrolyser} = \frac{\dot{m}_{H2}\ HHV}{\dot{W}_{in}}$

The electrolyser efficiency is assumed to be 60%.[9]

4. RESULTS AND DISCUSSION

The equations listed above were inserted into EES (Engineering Equations Solver) a widely used software package. The equations were run and a parametric analysis was performed on the different systems investigating the effects of several variables on performance and efficiency. The overall analysis off the whole system was achieved by combining the analysis of each subsystem. For the Solar receiver/heliostat field, the input variables needed for calculation are shown in Table 1. These parameters when inserted are used to calculate the amount of useful energy input to the molten salt, the surface temperature of the receiver, the amount of solar energy which is considered as the heat input to the receiver and the thermal efficiency of the receiver. The main results of this base study are listed in Table 2. Table 3 gives he properties at each state point.

Table 2. Properties of the Central receiver

Parameter	Symbol	Value
Surface temperature of the receiver	$T_{rec,surf}$	1050K
Energy efficiency of the receiver	$\eta_{En_{rec}}$	76.48%
Total heat received by the receiver	$\dot{Q}_{rec}$	9MW

4.1.1. Effect of ambient temperature on energy efficiency

One important parameter that affects the performance of most thermodynamic systems is the ambient temperature. The effect of the variations in ambient temperature on the energy efficiency of this system and its subsystems are shown in Fig 3. It is seen that as the ambient temperature increases from 270K to 320K, there is no obvious change in the energy efficiency of the system and its subsystem. This is due to the fact that the energy model does not put into consideration losses and irreversibility, unlike the exergy model that considers losses and irreversibility. This result is in confirmation with the results gotten by [4].

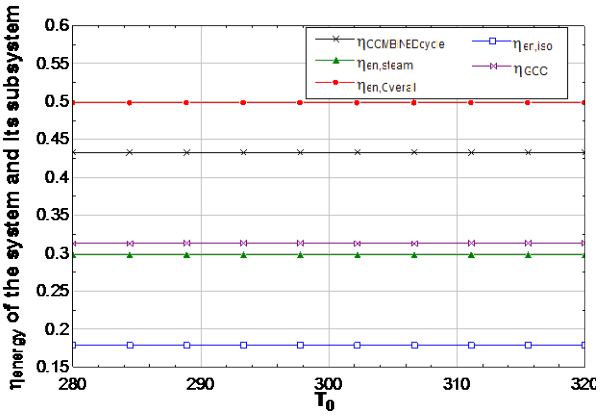

Figure 2: The variation with ambient temperature of the energy efficiency of the overall multigeneration system and its subsystems

4.1.2. Effect of solar radiation on work done and rate of hydrogen Produced

The solar radiation is important parameter that affects the performance of any solar system, because it determines the amount of solar energy available to be converted to power. The effect of the incident solar radiation on the work done by the system's sub-systems and the rate of hydrogen production is reported. It is seen that as the solar flux increases from 650W/m^2 to 1100W/m^2, work done by the gas turbine, steam turbine, organic Rankine cycle turbine increases almost linearly. The rate of hydrogen produced also increases. This is because the higher the solar energy available, more heat is converted to useful work.

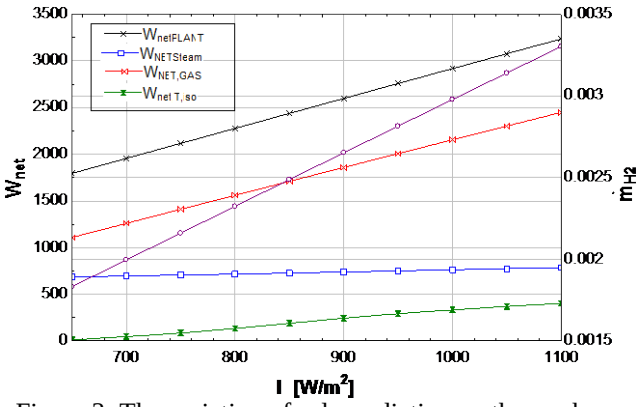

Figure 3: The variation of solar radiation on the work done of system and the rate of hydrogen produced.

4.1.3. Effect of solar field area on energy efficiency

The heliostat field area has very important effect on the multigeneration system because it has a relationship to the input energy and exergy. Fig 5 shows the effects of changing the aperture area on the energy efficiency of the multigeneration system and its subsystems. As the aperture area increases from 8000m^2 to 15000m^2, the efficiency of the gas cycle increased from 26.99% to 32.66%, while the steam cycle energy efficiency increased from 25.74 to 28.98%. The organic Rankine cycle efficiency increased from 7.3% to about 18% and later drops down to 16.36%, while the efficiency of the combined cycle declines from 43.36 to 41.92%. The overall energy efficiency is seen to increase from 43.54% to 52.22%, and the COP(en) decreases from about 0.8506 to 0.8363 this is because of the heat been added of the generator of the AC. As more heat is added the COP declines because of the fixed evaporator temperature.

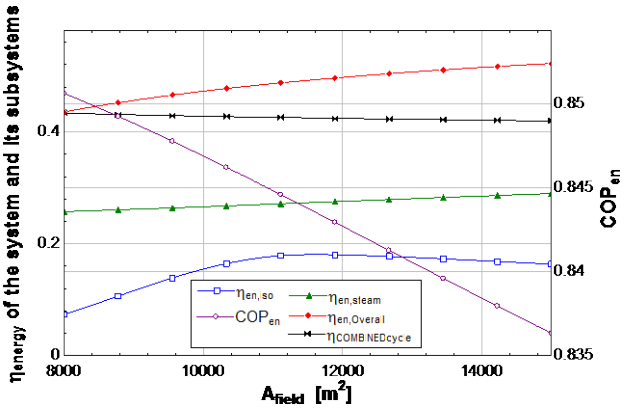

Figure 4: The variation of heliostat field area on the energy efficiency of the system and its subsystems.

4.1.4. Effect of generator temperature n COP(en) and exergy efficiency of the AC

Fig 9 displays the effect of temperature of the generator on the COP (en) and COP (ex) of the absorption cycle. As the generator temperature increases from 333.2K to 363.2K, the energetic COP reduces from 0.898 to 0.8231and the exegetic COP also reduces from 0.3681 to 0.3374. This is because he evaporator load is fixed. Therefore, for a fixed evaporator load, there is no significance of any additional heat been added to the generator. This behaviour is in line with the observation made by [10], when the increase in generator inlet temperature was plotted against the COP there was an inverse relation to the heat been added to the generator.

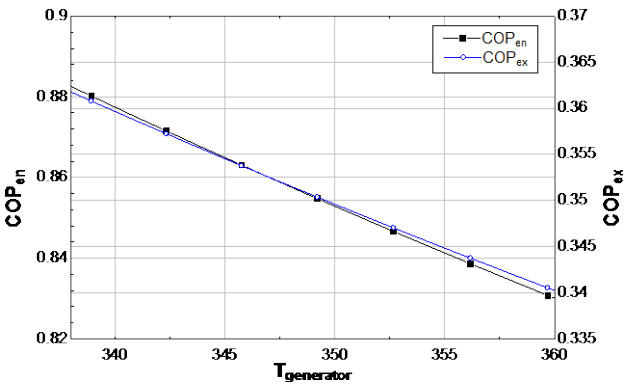

Figure 5: The variation with generator temperature on COP (en) and exergy efficiency of the AC

4.1.5. Effect of pressure ratio on work done by the gas turbine and the energy efficiency of the gas cycle

The pressure ratio is an important parameter in the design of gas power plants. The effect of pressure ratio on the net-work and thermal efficiency of the gas cycle in the multigeneration system is shown in the Fig 6 below. As the pressure ratio increases, the work done increases from 871.8kW to 2414kW and then declines at point where pressure ratio is 16. The efficiency also increases from 12.66% to 35.77%.

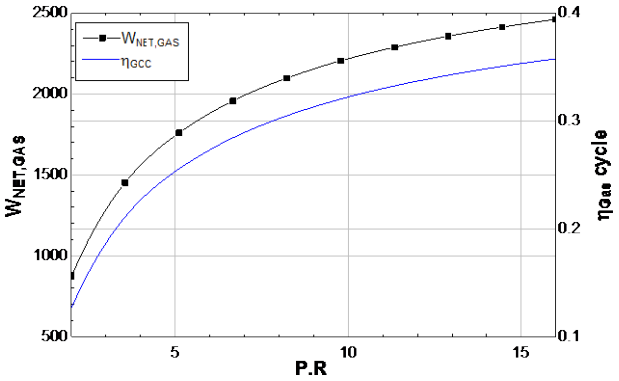

Figure 6: The variation of pressure ratio on the net-work and energy efficiency of the gas cycle.

5. CONCLUSIONS

This paper focuses on developing a novel multigeneration energy system using solar energy to generate power, heating and cooling. Thermodynamic analysis is performed so as to have a good understanding of the system. The system utilizes a Brayton cycle, Rankine cycle, an Organic Rankine cycle, absorption chiller, domestic hot water system and an electrolyser.

Table 3. Properties of each state point of the system

State Points	T (K)	P(kPa)	h (kJ/kg)	s (kJ/kg)	$\dot{E}x$ (kJ/kg)	$\dot{m}$ (kg/s)
1	298	101.3	298.4	5.695	0	9
2	598.4	911.9	605.6	5.775	2550	9
3	1278	911.9	1370	6.622	7162	9
4	801.4	101.3	823.8	6.719	1981	9
5	668	7000	3145	6.43	1056	0.8555
6	459.6	1000	2794	6.623	706	0.8555
7	668	1000	3144	7.451	794	0.8555
8	354.4	20	2594	7.863	218.6	0.8555
9	333.2	20	251.4	0.832	6.832	0.8555
10	333.9	7000	260.3	0.8374	13.06	0.8555
11	512.6	101.3	516.3	6.245	486.9	6
12	305	1	69.9	0.2085	3.061	5
13	305.5	4.81	69.9	0.2119	-2.026	5
14	343.5	4.81	151.9	0.4613	36.18	5
15	351.5	4.81	196.3	0.437	148.8	4.29
16	319.3	4.81	100.8	0.2556	-29.13	4.29
17	322	1	100.8	0.2715	-49.43	4.29
18	347.5	4.81	2707	8.653	94.21	0.7098
19	305.3	4.81	134.9	0.4669	0.1954	0.7098
20	280.1	1	134.9	0.1059	75.55	0.7098
21	280.5	1	2514	8.977	-111	0.7098
22	277.1	180	209.2	1.033	154	3
23	278.9	3000	215.3	1.038	168.4	3
24	437.5	3000	820.8	2.692	506	3
25	361.5	180	709.8	2.78	94.42	3
26	314	101.3	314.5	5.748	3.546	9
27	300	101.3	26.94	0.3928	-556.5	6.5
28	334.8	101.3	258	0.8514	57.04	6.5

The energy and exergy efficiencies of the gas cycle are observed to be 31.31% and 40.83% respectively**,** energy and exergy efficiencies of the steam cycle is 27.57% and 49.77% respectively**,** energy and exergy efficiencies of the combined cycle is 48.51% and 55.28% respectively**,** while the energy and exergy efficiencies of the overall multigeneration system is 49.74% and 27.12% respectively and for the organic Rankine cycle, the energy and exergy efficiency is 17.99% and 56.44%. The COP and exegetic efficiency of the absorption chiller is 0.8427 and 0.3454 respectively, while the cooling capacity of the absorption chiller is 1689kW and heating capacity of the domestic water heater is 1502kW.

Further findings of the present study are listed below:

- Environmental parameters like the ambient temperature and solar irradiation influence the performance of the system.
- High concentration ratio of the heliostat field, pressure ratio in the gas cycle, lower absorption cycle evaporating temperature and condensation temperatures are needed to provide good energetic and energetic performance of the system.
- It can be seen from the results that the system's energy efficiency increases with multigeneration. The multigeneration technique is, therefore, a very ground-breaking idea. It improves system efficiency, saves cost and helps reduce the effect of global warming. Its becomes highly sustainable when the sources used are renewable energy sources.

Nomenclature

AC	Absorption Chiller
insi	insulation
F_r	View factor
C	Concentration ratio
ORC	Organic rankine cycle

Greek Letters

ε	Emissivity
ρ	Density
σ	Stefan-Boltzmann constant
λ	Thermal conductivity

References

[1] Siddiqui, O. and Dincer, I. (2018). Examination of a new solar-based integrated system for desalination, electricity generation and hydrogen production. *Solar Energy*, 163, pp.224-234.

[2] Nzihou A, Flamant G, Stanmore B. Synthetic fuels from biomass using concentrated solar energy – a review. Energy 2012;42:121–31.

[3] Dincer, I. and Zamfirescu, C. (2012). Renewable-energy-based multigeneration systems. *International Journal of Energy Research*,**36**(15), pp.1403-1415.

[4] Khalid, F., Dincer, I. and Rosen, M. (2015). Energy and exergy analyses of a solar-biomass integrated cycle for multigeneration. *Solar Energy*, 112, pp.290-299.

[5] Ozlu, S. and Dincer, I. (2016). Performance assessment of a new solar energy-based multigeneration system. *Energy*, 112, pp.164-178.

[6] Hogerwaard, J., Dincer, I. and Naterer, G. (2017). Solar energy based integrated system for power generation, refrigeration and desalination. *Applied Thermal Engineering*, 121, pp.1059-1069.

[7] Rabbani, M., Ratlamwala, T. and Dincer, I. (2017). Development of a New Heliostat Field-Based Integrated Solar Energy System for Cogeneration. *Arabian Journal for Science and Engineering*.

[8] Shahin, M., Orhan, M. and Uygul, F. (2016). Thermodynamic analysis of parabolic trough and heliostat field solar collectors integrated with a Rankine cycle for cogeneration of electricity and heat. *Solar Energy*, 136, pp.183-196.

[9] Almahdi, M., Dincer, I. and Rosen, M. (2016). A new solar based multigeneration system with hot and cold thermal storages and hydrogen production. *Renewable Energy*, 91, pp.302-314.

[10] Badri & Khadka, Roshan. (2012). Design and analysis of solar absorption air cooling system for an office building